ARID ZONE JOURNAL OF ENGINEERING, TECHNOLOGY & ENVIRONMENT
AZOJETE September 2026. Vol.22(3):592-607
Published by the Faculty of Engineering, University of Maiduguri, Maiduguri, Nigeria.
**Print ISSN: 1596-2490, Electronic ISSN: 2545-5818**
https://doi.org/10.63958/AZOJETE/2026/22/03/004
www.azojete.com.ng

ORIGINAL RESEARCH ARTICLE

# HYBRID INCREMENTAL CONDUCTANCE–MODEL PREDICTIVE CONTROL FOR MAXIMUM POWER POINT TRACKING UNDER VARYING IRRADIANCE AND TEMPERATURE CONDITIONS

**M.A. Jada[1,2*], M. Musa[1,5], S. Ibrahim[3], T.A. Aljazuli [4], Y. Hassan [6]**

[1]*Department of Electrical Engineering, Ahmadu Bello University, Zaria, Kaduna State, Nigeria.*
[2]*Department of Electrical & Electronic Engineering Technology, Adamawa state Polytechnic, Yola, Adamawa State, Nigeria.*
[3]*Department of Electrical and Electronics Engineering, Edo State University, Iyamho. Edo State, Nigeria*
[4]*Department of Electrical & Electronic Engineering Technology, Federal Polytechnic, Mubi, Adamawa State, Nigeria.*
[5]*Kaduna State Power Supply Company (KAPSCO), Kaduna State, Nigeria.*
[6]*Department of Computer Science, University of the People, America.*
**Corresponding author's Email: mabduljada@gmail.com*

**ARTICLE INFORMATION**

**Received: 23rd May 2026**
**Revised: 4th August 2026**
**Accepted: 6th August 2026**

**Keywords:**
*Photovoltaic (PV)*
*Maximum power point tracking (MPPT)*
*Incremental conductance*
*Model predictive control*
*Hybrid MPPT*
*MATLAB/Simulink*

**ABSTRACT**

*Photovoltaic systems experience variations in irradiance and temperature that continuously shift the maximum power point, making effective MPPT essential for maximizing energy extraction. Conventional methods such as Perturb and Observe and Incremental Conductance are simple to implement but may suffer from slow convergence, oscillations, and reduced accuracy under rapidly changing conditions. Model Predictive Control offers faster dynamic response but at the cost of higher computational requirements. This study developed a hybrid Incremental Conductance–Model Predictive Control algorithm for photovoltaic MPPT. The Incremental Conductance stage generated the reference voltage, while the finite-control-set predictive controller selected the switching state of the boost converter that minimized the voltage-tracking error. The controller was implemented in MATLAB/Simulink and evaluated at irradiance levels of 1000, 800 and 500 W/m², with cell temperatures ranging from 25°C to 35°C. Its performance was compared with that of a conventional Perturb and Observe–Model Predictive Control method. The proposed controller achieved a tracking efficiency of 98.8%, compared with 96.9% for the conventional controller. In addition, the overall settling time decreased from 100 ms to 70 ms, while the steady-state power oscillation was reduced from 8.5 W to 2.3 W. Similarly, the controller was observed to have produced lower overshoot and a faster rise time. These simulation results show that the hybrid IN-MPC method improved energy extraction, transient response and steady-state stability under the investigated operating conditions. However, this study recommends both eexperimental and hardware-based studies to confirm its real-time performance.*



## 1.0 Introduction

Photovoltaic (PV) energy has become an important component of renewable electricity generation because it is clean, modular and relatively easy to maintain. However, the electrical behaviour of a PV module is nonlinear and depends strongly on solar irradiance, cell temperature and load conditions. Changes in these variables shift the operating point of the module and alter the maximum power available from the PV array (Motahhir *et al*., 2020; Kumar *et al*., 2022). A maximum power point tracking (MPPT) technique is, therefore, needed to regulate the operating point to improve energy extraction under changing environmental conditions.

Perturb and Observe (PO) and Incremental Conductance (IC) are one of the most commonly used MPPT techniques due to the fact that they require relatively simple control procedures and limited computational resources. The PO method determines the direction of the maximum power point (MPP) by introducing small changes to the operating voltage. Although the technique is simple to implement but normally produces oscillations around the MPP and may select an incorrect tracking direction when irradiance changes rapidly (Abdel-Salam *et al.,* 2018). Incremental Conductance improves tracking by using the relationship between incremental and instantaneous conductance (Abdel-Salam *et al.,* 2018). Nevertheless, its performance depends on the selected step size, sampling conditions, and residual oscillations or delayed convergence may still occur under highly dynamic operating conditions (Abdel-Salam *et al*., 2018; Al-Wesabi *et al.,* 2024).

Artificial Neural Networks (ANN), Genetic Algorithms (GA), Particle Swarm Optimization (PSO) and Fuzzy Logic Control have also been applied to PV MPPT. These methods can adapt to nonlinear operating conditions and, in some applications, provide better tracking accuracy than conventional algorithms (Kumar *et al*., 2022). Their implementation, however, may require training data, parameter tuning, optimization procedures or additional computational resources. Such requirements can increase design complexity and limit their use in low-cost PV controllers (Alshareef *et al*., 2021; Kumar *et al*., 2022).

Advanced nonlinear and predictive controllers have been introduced for the improvement of the dynamic behaviour of an MPPT system. Sliding Mode Control offers strong robustness but may suffer from chattering. Backstepping control provides systematic nonlinear control but generally involves a more demanding mathematical design (Bhagwan *et al*., 2024). Again, Model Predictive Control (MPC) predicts the response of the power converter and selects a control action that minimizes a specified objective function. This enables rapid transient response and direct control of converter switching states. However, repeated prediction and optimization at every sampling interval may impose a considerable computational burden, particularly when the prediction model or objective function is complex (Rivera *et al*., 2021; Bhagwan *et al.,* 2024).

Recent studies have combined conventional MPPT methods with nonlinear, intelligent or predictive controllers to obtain the advantages of more than one technique (Bollipo *et al*; (2020); Worku *et al*; (2023); Endiz *et al*; (2025)). Incremental Conductance has, for example, been integrated with integral backstepping and sliding-mode controllers to improve convergence and robustness. Although these approaches have reported improved performance, their control structures may become complex, while sliding-mode implementations may still experience chattering (Harrison *et al*., (2023); Messaoudi *et al.,* 2024). Other hybrid MPPT methods have also achieved high tracking efficiencies, but many require extensive tuning, optimization or additional computational effort (Bouzid *et al*., 2020). The literature, therefore, shows an important trade-off between tracking accuracy, convergence speed, steady-state stability and implementation complexity (Endiz *et al*; 2025; Worku *et al*; 2023). Conventional methods are computationally economical but may respond poorly to rapid operating changes, whereas advanced control methods usually provide better dynamic performance at the cost of greater complexity. A practical MPPT controller should respond rapidly to irradiance and temperature variations, maintain operation close to the MPP and limit steady-state oscillations without relying on an excessively complicated control structure.

To address this requirement, this study proposes a hybrid Incremental Conductance–Model Predictive Control technique. The IC component determines the reference voltage associated with the MPP, while the finite-control-set MPC predicts the response of the DC–DC boost converter and selects the switching state that minimizes the voltage-tracking error. The proposed controller is evaluated under different irradiance and temperature conditions and compared with a conventional Perturb and Observe–Model Predictive Control (PO-MPC) approach. The study specifically examines tracking efficiency, settling time, dynamic response and steady-state oscillation.

## 2. Materials and Method

### 2.1 Research Methodology

A simulation study was conducted to develop and evaluate the proposed hybrid Incremental Conductance–Model Predictive Control (IN-MPC) technique for MPPT in a PV system. The control system was implemented in MATLAB/Simulink by combining the reference-voltage estimation process of the IC algorithm with the switching-state selection capability of Finite-Control-Set Model Predictive Control (FCS-MPC) (MathWorks, 2024).

The simulated system comprised a PV module, a boost converter, voltage and current measurement units, the IN-MPC controller and a resistive load. The IC algorithm used the measured PV current and voltage to estimate the reference voltage at the MPP. The predictive controller then evaluated the possible switching states of the boost converter and select the state that produced the smallest deviation from the reference voltage. The basic predictive-control procedure followed the principles described by Rodriguez and Cortes, (2012) and Vazquez *et al*; (2017).

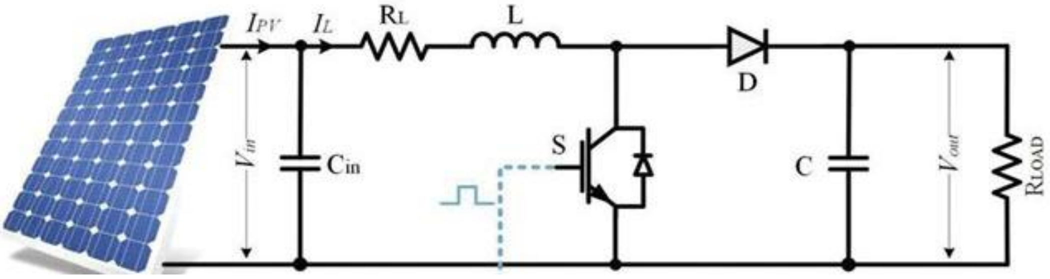


**Figure 1**: Configuration of the Proposed PV System with the Hybrid IN-MPC Controller (adapted from Vazquez *et al*., 2017).

The controller was tested under different irradiance levels of 1000, 800 and 500 W/m², with operating temperatures between 25°C and 35°C. These conditions were selected to examine the strenght of the controller to respond to changes in the available PV power.

The performance of the proposed controller was compared with that of a conventional PO-MPC method. Both controllers were evaluated using the same PV model, boost-converter parameters, environmental inputs and load conditions. The principal performance indicators were tracking efficiency, settling time, dynamic response and steady-state power oscillation. These measures were commonly used to assess the tracking accuracy and transient behaviour of MPPT controllers (Esram & Chapman, 2007; Motahhir *et al.,* 2020).

### 2.2 Photovoltaic-System Architecture

The PV array was represented using the single-diode equivalent-circuit model. This model was selected because it provides a practical representation of the nonlinear current–voltage behaviour of a PV module without requiring an excessively complex mathematical structure. It has been widely applied in PV simulation and MPPT studies (De Soto *et al*., 2006; Villalva *et al*., 2009).

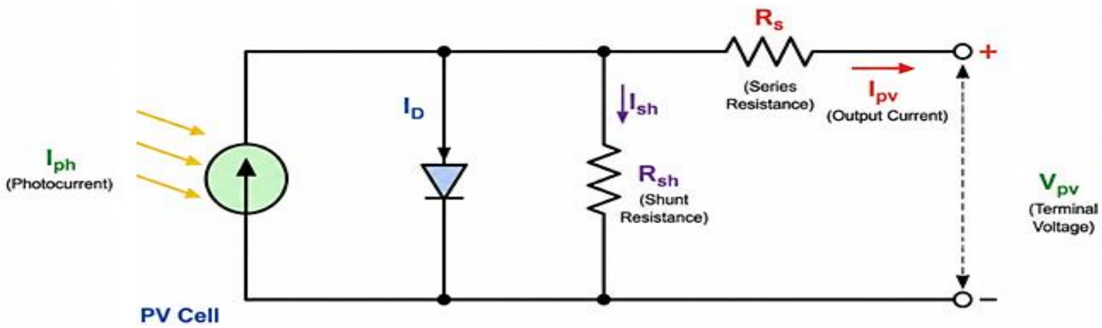


**Figure 2**: Single-Diode Equivalent Circuit Model of the PV Cell (Villalva *et al.,* 2009).

As shown in Figure 2, The equivalent model comprises of a photogenerated current source, a diode, and two resistive elements representing the series and shunt resistances. The photocurrent source models the electrical current generated when solar irradiance falls on the PV cell. The diode models the photovoltaic cell's semiconductor junction, whereas the series resistance reflects the internal losses that resist electrical current flow. The shunt resistance represents leakage-current paths within the cell.

The PV output current is expressed as in (Villalva *et al.,* 2009):

$$I_{pv} = I_{ph} - I_0\left[\exp\left(\frac{q\left(V_{pv} + I_{pv}R_s\right)}{nkT}\right) - 1\right] - \frac{V_{pv} + I_{pv}R_s}{R_{sh}} \qquad 1$$

Here, $I_0$ denotes the diode reverse-saturation current in amperes, $q$ represents the elementary electron charge ($1.602 \times 10^{-19}$ C), and $n$ is the diode ideality factor, typically within the range $1 \le n \le 2$. The symbol $k$ refers to Boltzmann's constant ($1.381 \times 10^{-23}$ J/K), while $T$ represents the cell temperature in kelvin. In addition, $R_s$ and $R_{sh}$ denote the series and shunt resistances, respectively, both measured in ohms ($\Omega$).

The generated photocurrent depends mainly on irradiance, although it is also affected by cell temperature. It is calculated as in (Villalva *et al.,* 2009):

$$I_{ph} = \left[I_{sc,ref} + K_i\left(T - T_{ref}\right)\right]\frac{G}{G_{ref}} \quad 2$$

In this expression, $I_{sc,\mathrm{ref}}$ denotes the short-circuit current measured under Standard Test Conditions, while $K_i$ represents the temperature coefficient associated with the short-circuit current. The variables $G$ and $G_{\mathrm{ref}}$ refer to the incident solar irradiance and the standard reference irradiance of $1000\ \mathrm{W/m^2}$, respectively.

The instantaneous power produced by the PV module is given as in (Motahhir *et al*., 2020):

$$P_{pv} = V_{pv} I_{pv} \quad 3$$

where $P_{pv}$, $V_{pv}$ and $I_{pv}$ represent the PV power, voltage and current, respectively.

Because irradiance and temperature affect both the voltage and current of the array, they also change the position of the MPP. An MPPT controller is therefore required to regulate the operating point whenever environmental conditions change (Esram and Chapman, 2007).

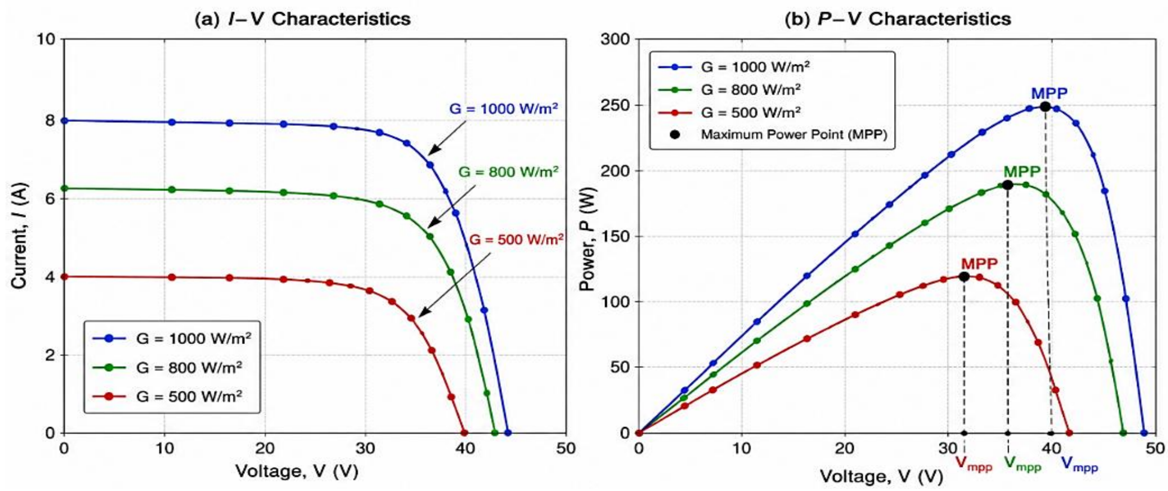


**Figure 3**: Current–Voltage and Power–voltage Characteristics of the PV Module at Different Irradiance Levels (adapted from Villalva *et al*., 2009).

Figure 3 shows that increasing irradiance raises the PV current and the maximum available power. Temperature changes mainly affect the output voltage and consequently alter the position of the MPP. The single-diode model was used to assess the tracking accuracy, convergence behaviour, transient response and steady-state performance of the proposed IN-MPC controller.

### 2.3 Design of the Proposed Hybrid IN-MPC Technique

The proposed IN-MPC technique combines two complementary control functions. The IC algorithm estimates the reference voltage associated with the MPP, while the Finite-Control-Set Model Predictive Controller determines the most suitable switching state of the boost converter. This arrangement separates MPP estimation from converter switching control to enables the controller to respond quickly to changes in irradiance and temperature.

The IC method is based on the slope of the PV power–voltage curve. At the MPP (Motahhir *et al*., 2020),

$$\frac{dP}{dV} = 0 \qquad 4$$

Since PV power is given as in (Motahhir *et al*., 2020):

$$P = VI \qquad 5$$

differentiating Equation (5) with respect to voltage gives

$$\frac{dP}{dV} = I + V\frac{dI}{dV} \qquad 6$$

At the MPP,

$$I + V\frac{dI}{dV} = 0 \qquad 7$$

Therefore,

$$\frac{dI}{dV} = -\frac{I}{V} \qquad 8$$

The operating region of the PV array is determined by comparing IC, $dI/dV$, with instantaneous conductance, $-I/V$. When

$$\frac{dI}{dV} > -\frac{I}{V} \qquad 9$$

the operating region lies to the left of the MPP. The reference voltage is therefore increased. Conversely, when (Motahhir *et al*., 2020):

$$\frac{dI}{dV} < -\frac{I}{V} \qquad 10$$

the operating region lies to the right of the MPP, and the reference voltage is minimized. At the MPP,

$$\frac{dI}{dV} = -\frac{I}{V} \qquad 11$$

and the reference voltage remains unchanged (Motahhir *et al*., 2020).

The reference voltage obtained from the IC algorithm is supplied to the FCS-MPC stage. Using a discrete-time model of the boost converter, the predictive controller estimates the PV voltage for each permissible switching state during the next sampling interval. The predicted values are then compared with the reference voltage, and the switching state with the smallest voltage-tracking error is selected (Rodriguez *et al.,* 2013; Vazquez *et al*., 2017).

The cost function is defined as in (Motahhir *et al*., 2020):

$$g_s = \left|V_{\text{ref}}(k) - V_{\text{pred},s}(k+1)\right| \qquad 12$$

where $g_s$ is the cost associated with switching state $s$, $V_{\text{ref}}(k)$ is the reference voltage generated by the IC algorithm, and $V_{\text{pred},s}(k+1)$ is the predicted PV voltage for the corresponding switching state.

The optimal switching state is selected as in (Motahhir *et al*., 2020):

$$s^* = \arg\min_{s \in S}(g_s) \qquad 13$$

where $S$ represents the set of feasible converter switching states and $s^*$ is the state that produces the minimum predicted voltage error.

The selected state is applied directly to the converter during the next sampling interval. Unlike a conventional arrangement that passes the MPPT output through a separate pulse-width modulation stage, the predictive controller evaluates the available switching options and applies the preferred action according to the converter model. This process is repeated at every sampling instant, allowing the operating voltage to remain close to the maximum-power-point reference.

By combining Incremental Conductance reference generation with predictive switching control, the proposed method is intended to reduce convergence time and steady-state oscillation while maintaining accurate tracking during changes in operating conditions.

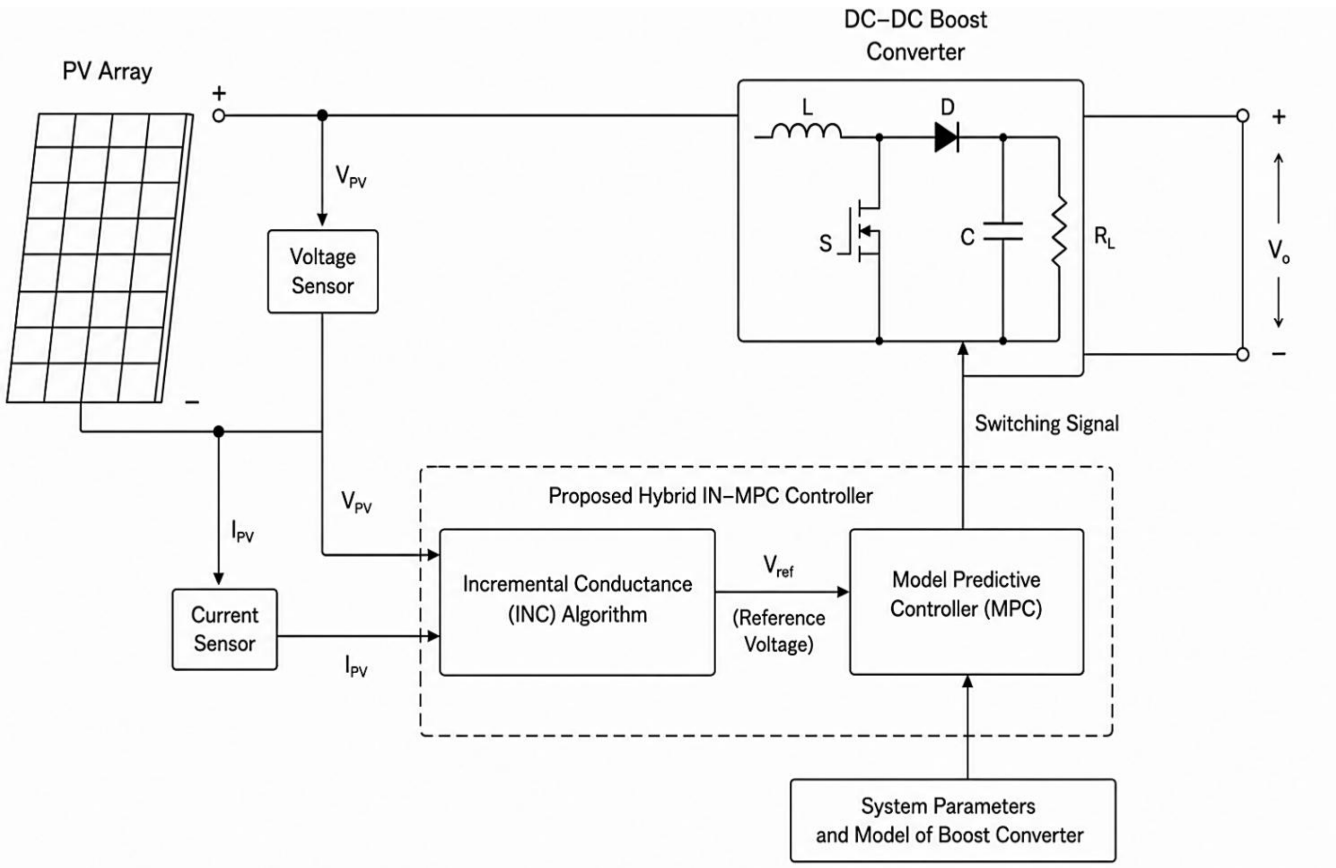


**Figure 4**: Block Diagram of the Proposed Hybrid IN-MPC Architecture.

Figure 4 presents the main signal flow within the proposed controller. The PV voltage and current are supplied to the IC block, which generates $V_{\text{ref}}$. The predictive controller uses this reference, together with the boost-converter model and measured system variables, to determine the switching command applied to the converter.

As illustrated in Figure 5, the control procedure begins with the measurement of PV voltage and current. The corresponding incremental values are calculated and used to update the reference voltage. The predictive stage then estimates the voltage response for each feasible switching state, evaluates the cost function and applies the state with the lowest tracking error. The measured variables are subsequently updated, and the procedure continues during the next sampling interval.

## 2.4 Mathematical Model of the DC–DC Boost Converter

The boost converter which connects the PV module to the load controls the operating voltage of the array. By changing its switching state, the converter regulates energy transfer from the PV source and enables the MPPT controller to move the operating point towards the MPP. The boost topology was selected because of its simple structure, voltage step-up capability and widespread application in PV conversion systems (Rashid, 2018, pp. 215–250; Villalva *et al.*, 2009).

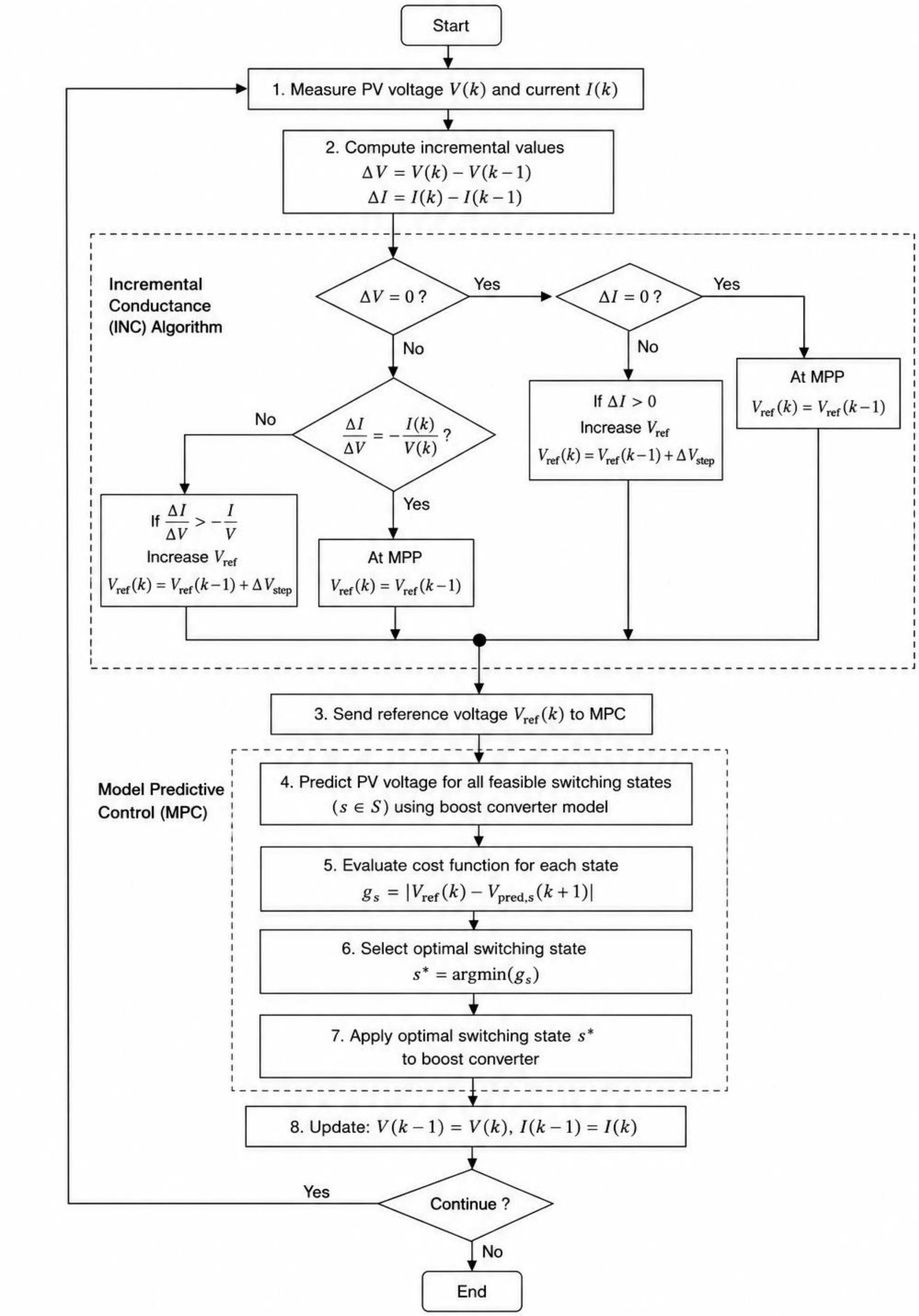


**Figure 5**: Flowchart Diagram of the Proposed Hybrid IN-MPC Technique.

The converter comprises an inductor $L$, a semiconductor switch $S$, a diode $D$, an output capacitor $C$ and a load resistance $R_L$. Its dynamic behaviour depends on whether the switch is in the ON or OFF state.

### 2.4.1 Switch-ON State

When the switch is in the ON state, the diode is reverse-biased and the PV array sends energy to the inductor device. During this interval, the capacitor supports the load. The boost converter equations as in (Villalva *et al.*, 2009)

$$\frac{di_L}{dt} = \frac{V_{PV}}{L} \quad 14$$

and

$$\frac{dV_o}{dt} = -\frac{V_o}{R_L C} \quad 15$$

where $i_L$ is the inductor current, $V_{PV}$ is the PV array voltage and $V_o$ is the converter output voltage.

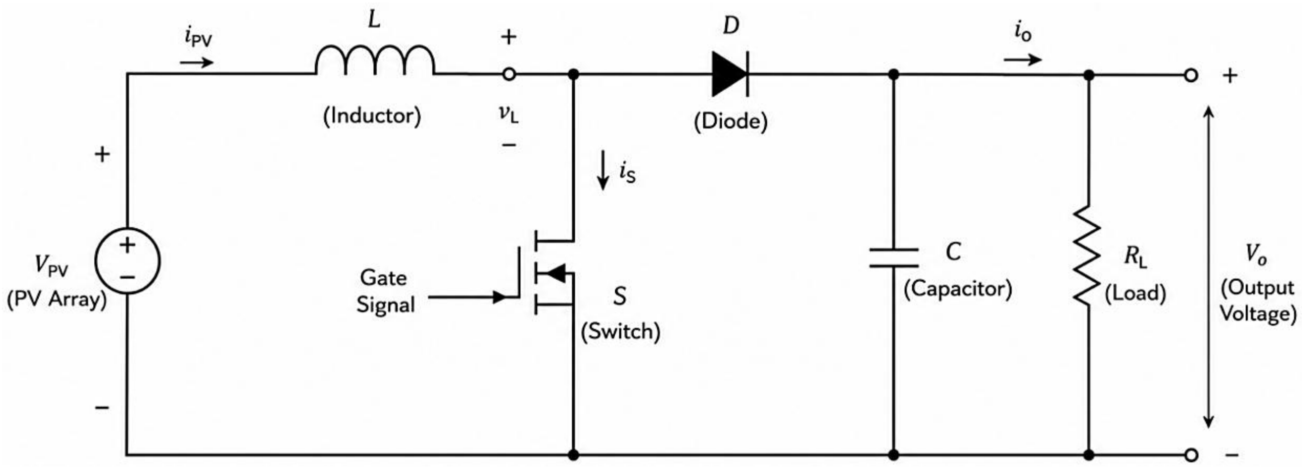


**Figure 6**: Schematic Diagram of the Boost Converter used in the Photovoltaic System (Villalva *et al*., 2009).

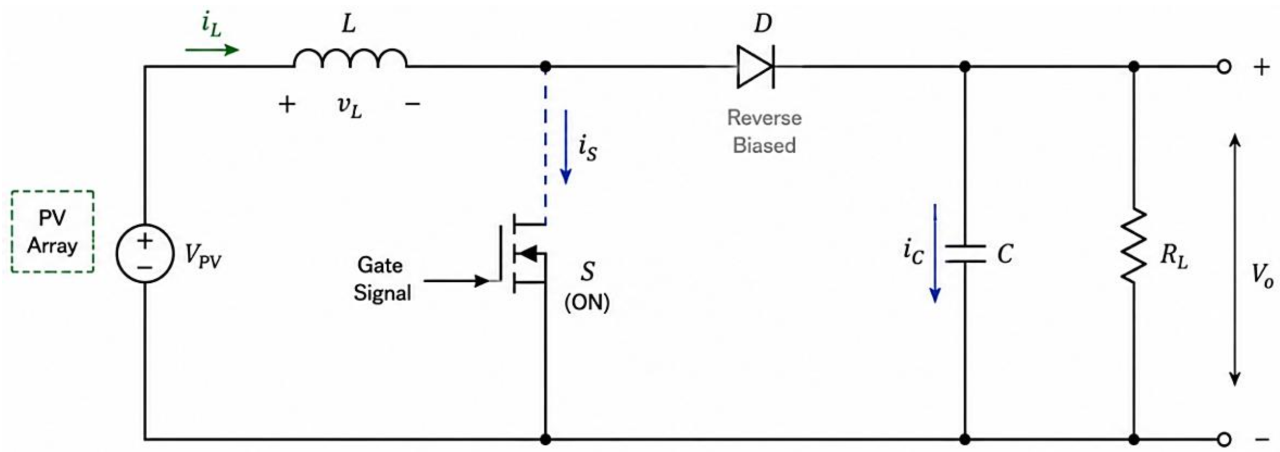


**Figure 7**: Equivalent Converter Circuit when the Power Switch is ON (Motahhir *et al*., 2020)

### 2.4.2 Switch-OFF State

When the switch is in the OFF state, the inductor discharges its retained energy through the diode to the capacitor and load. The system dynamics are expressed as in (Motahhir *et al*., 2020):

$$\frac{di_L}{dt} = \frac{V_{PV} - V_o}{L} \quad 16$$

and

$$\frac{dV_o}{dt} = \frac{i_L}{C} - \frac{V_o}{R_L C} \quad 17$$

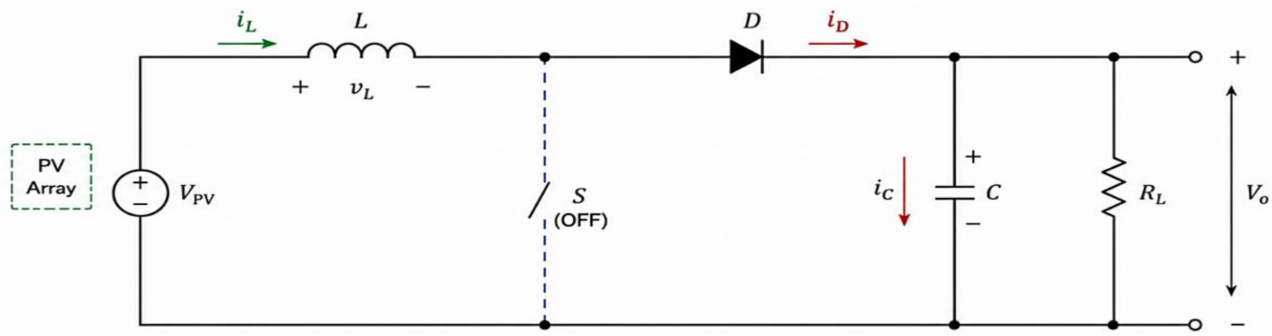


**Figure 8**: Equivalent Converter Circuit when the Power Switch is OFF (Motahhir *et al.*, 2020)

Equations (14 – 17) describe the continuous-time behaviour of the converter in its two switching states. For implementation of the predictive controller, these equations were converted into discrete-time form. The resulting model is used to estimate the future converter response for each switching option and to determine the state which minimizes the voltage-tracking error at every sampling interval. This model-based switching process supports rapid transient control and stable operation near the MPP (Rodriguez & Cortes, 2012; Vazquez *et al.*, 2017).

For an ideal boost converter operating under steady-state conditions, the connection between the input and output voltages is given as in (Motahhir *et al.*, 2020):

$$V_o = \frac{V_{PV}}{1 - D} \quad (18)$$

where $D$ is the converter duty ratio. An increase in $D$ raises the output voltage and changes the input impedance observed by the PV array. Through this relationship, the controller adjusts the array operating voltage and maintains operation near the MPP.

### 2.5 Simulation Setup and Performance Evaluation

The proposed IN-MPC controller was implemented in Simulink using the PV model, DC–DC boost converter, Incremental Conductance reference generator, predictive-control block, measurement units and resistive load described in the preceding sections. The simulation model was arranged to measure the PV voltage and current, calculate the reference voltage and determine the switching command applied to the boost converter.

In Figure 9, the PV array supplies the load through the boost converter. The measured array voltage and current are passed to the IC stage, which estimates the voltage corresponding to the MPP. The predictive controller uses this reference and the discrete-time converter model to evaluate the available switching states. The state giving the lowest predicted voltage error is then applied to the converter.

The PV module parameters used in the simulation are presented in Table 2, while Table 3 gives the principal converter and controller settings. These values were kept unchanged for both the proposed IN-MPC and conventional PO-MPC controllers to provide a consistent basis for comparison.

**Table 2**: Electrical parameters of the Canadian Solar PV module (Adapted from Ahmed *et al.*, 2017)

| Parameter | Symbol | Value | Unit |
|---|---|---|---|
| Maximum power at STC | $P_{mpp}$ | 410 | W |
| Open-circuit voltage | $V_{oc}$ | 68 | V |
| Short-circuit current | $I_{sc}$ | 7.84 | A |
| Voltage at MPP | $V_{mpp}$ | 63 | V |
| Current at MPP | $I_{mpp}$ | 6.5 | A |
| Number of series-connected modules | $N_s$ | 60 | — |
| Number of parallel strings | $N_p$ | 1 | — |
| Reference temperature | $T_{ref}$ | 25 | °C |
| Reference irradiance | $G_{ref}$ | 1000 | W/m² |

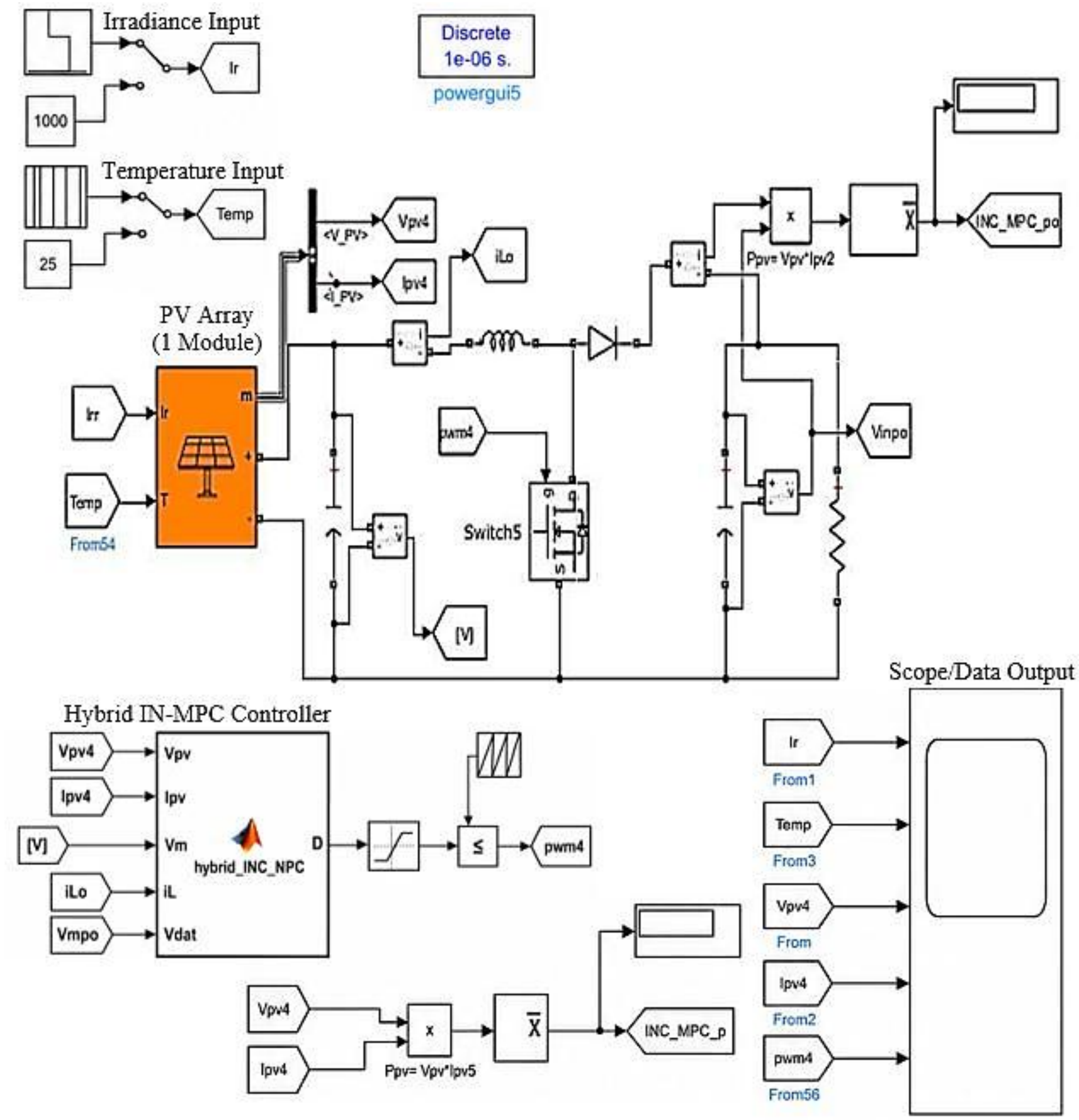


**Figure 9**: Simulink Model of the Proposed hybrid IN-MPC MPPT Controller.

**Table 3:** Boost converter and controllers design parameters

| Design parameter | Symbol | Value | Unit |
|---|---|---|---|
| Inductance | $L$ | 5 | mH |
| Output capacitance | $C$ | 1000 | μF |
| Load resistance | $R_L$ | 30 | Ω |
| MPC sampling time | $T_s$ | 15 | μs |
| INC sampling time | $T_{INC}$ | 100 | μs |
| INC voltage step | $\Delta V_{step}$ | 0.1 | V |
| Weighting factor | $\lambda$ | 0.1 | — |
| Prediction horizon | $N_p$ | 1 | — |
| Simulation duration | $t_{sim}$ | 3 | s |

The controllers were tested using step changes in irradiance to represent sudden variations in solar input. The irradiance was changed among 1000, 800 and 500 W/m², the cell temperature was varied between 25°C and 35°C. These operating points were implemented to assess the controllers under high, medium and low irradiance conditions.

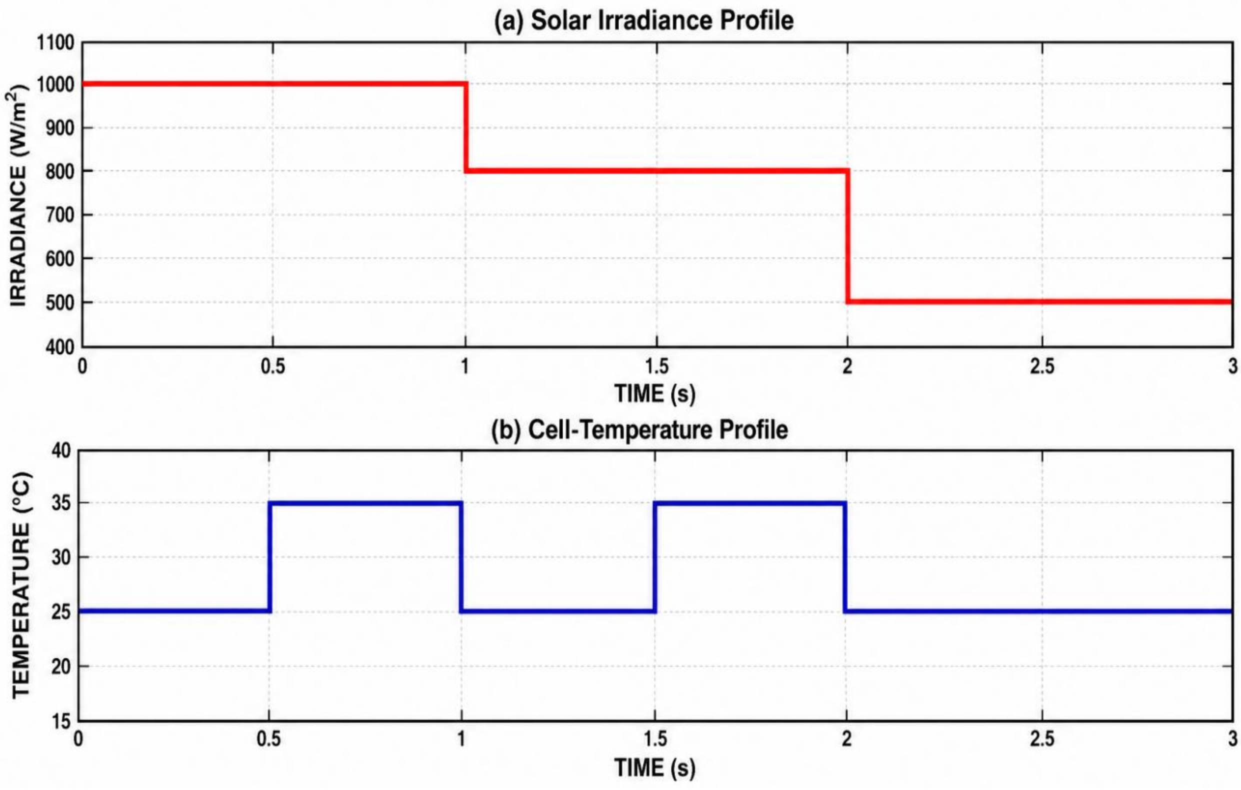


**Figure 10**: Irradiance and Cell-Temperature Profiles used for Evaluating the MPPT Controllers.

The IN-MPC and PO-MPC controllers were simulated under the same PV array, converter, load, sampling and environmental conditions. Their performance was evaluated using tracking efficiency, tracking error, settling time, rise time, maximum overshoot and steady-state power oscillation. These indices provide measures of energy extraction, transient speed and operating stability (Esram and Chapman, 2007; Motahhir *et al.,* 2020).

The MPPT efficiency was calculated from the ratio of the power extracted by the controller to the peak power available over the simulation interval:

$$\eta_{\mathrm{MPPT}} = \frac{\int_0^T P_{PV}\,(t)\,dt}{\int_0^T P_{MPP}\,(t)\,dt} \times 100\% \tag{19}$$

where $\eta_{\mathrm{MPPT}}$ is the tracking efficiency, $P_{PV}(t)$ is the power extracted from the PV array, $P_{MPP}(t)$ is the maximum power available at the prevailing irradiance and temperature, and $T$ is the simulation period.

The instantaneous difference between the available maximum energy and the extracted PV energy was determined as

$$e_p(t) = P_{MPP}(t) - P_{PV}(t) \tag{20}$$

where $e_p(t)$ represents the instantaneous power-tracking error. A smaller value indicates that the controller is operating closer to the MPP.

Settling time was taken as the period needed for the PV output to enter and stay within its steady operating range after an irradiance or temperature change. Rise time measured the initial speed of response, while maximum overshoot represented the largest temporary departure from the final operating value. Steady-state oscillation was evaluated from the remaining power variation after the controller had settled.

The resulting voltage, current and power responses were examined to determine whether the proposed IN-MPC controller provided faster convergence, improved energy extraction and lower oscillation than the conventional PO-MPC method.

## 3. Results and Discussion

The proposed IN-MPC controller and the conventional PO-MPC controller were evaluated under the same conditions as stated earlier. Their responses were compared using tracking efficiency, tracking error, settling time, rise time, maximum overshoot and steady-state power variation to be able to carry out a fair comparison.

### 3.1 Performance under Changes in Irradiance

The irradiance profile used for the simulation was varied in steps from 1000 W/m² to 800 W/m² and then to 500 W/m². These changes represented reductions in the solar energy received by the PV array and produced corresponding shifts in the available maximum power.

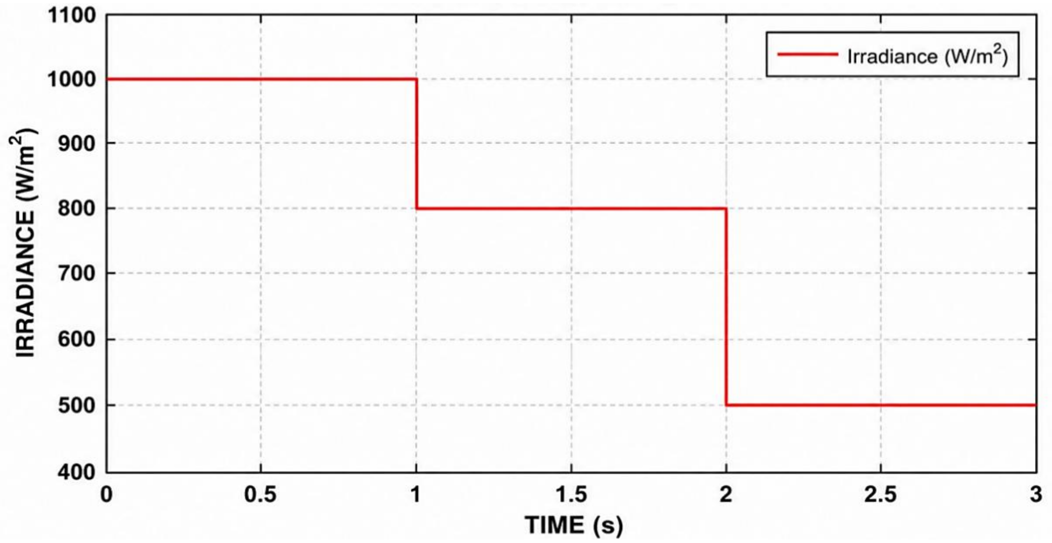


**Figure 11**: Stepwise Irradiance Profile used to Evaluate the Proposed IN-MPC and Conventional PO-MPC Controllers.

At each irradiance transition, the controllers were required to relocate the MPP and regulate the boost converter at the new operating condition. The reduction in irradiance lowered the PV current and available output power. Consequently, the controller response after each transition provided a basis for assessing convergence speed, tracking accuracy and steady-state stability.

Both controllers responded to the applied changes and maintained operation within the expected PV operating range. However, the proposed IN-MPC controller generally reached the new operating point more quickly and with less variation after the transient period.

### 3.2 Dynamic Response of the Controllers

Figure 12 compares the output power, PV voltage and current obtained with the two control methods. The power responses in Figure 12(a) show that both controllers followed the changes in available PV power. The proposed IN-MPC response, however, approached the new power level more rapidly and showed smaller fluctuations around the operating point. This behaviour was more noticeable immediately after the step changes in irradiance.

The voltage responses in Figure 12(b) indicate that the proposed controller maintained the PV voltage closer to its reference value. This resulted from the use of IC to update the MPP voltage and the predictive stage to select the converter switching action.

A similar response was observed for the PV current in Figure 12(c). The current changed with each irradiance level, but the IN-MPC controller produced a more stable response after the transient interval. The lower voltage and current variations also contributed to the reduced power oscillation recorded for the proposed controller.

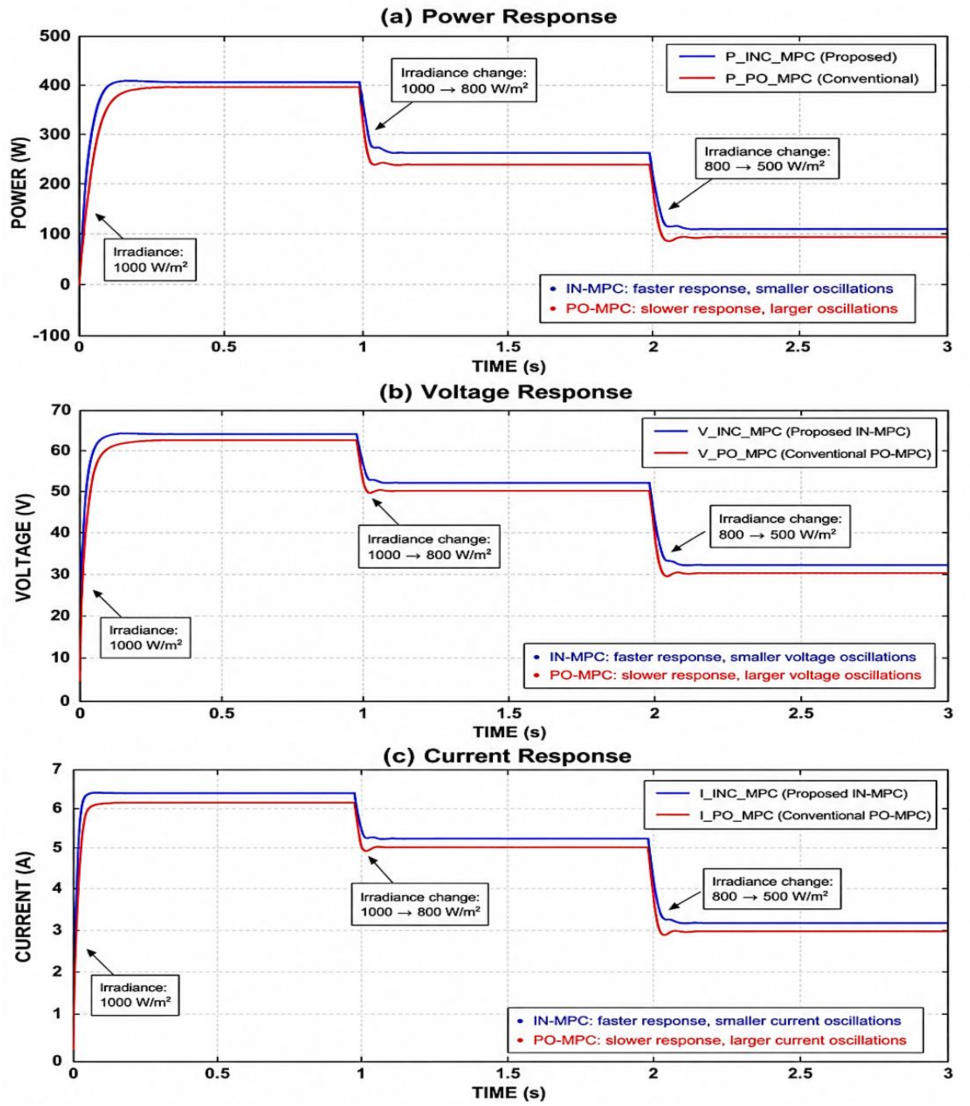


**Figure 12:** Dynamic Responses of the Conventional PO-MPC and Proposed IN-MPC Controllers: (a) PV power, (b) PV voltage and (c) PV current response.

The improvement can be explained by the functions assigned to the two parts of the hybrid controller. The IC stage determines the direction in which the operating voltage should be adjusted, while the predictive stage evaluates the possible converter actions before applying a switching command. The PO-MPC controller, in contrast, obtains its reference through repeated perturbation. This process can produce additional movement around the operating point, particularly after the MPP has been reached.

### 3.3 Comparative Performance Analysis

Table 4 presents the settling times and tracking errors obtained under the investigated irradiance and temperature conditions.

**Table 4:** Performance of the IN-MPC controller relative to the conventional PO-MPC controller

| Operating condition | PO-MPC settling time (s) | IN-MPC settling time (s) | Time reduction (s) | PO-MPC tracking error (%) | IN-MPC tracking error (%) | Error reduction (percentage points) |
|---|---|---|---|---|---|---|
| 1000 W/m², 25°C | 0.23 | 0.16 | 0.07 | 3.6 | 2.7 | 0.9 |
| 1000 W/m², 35°C | 0.50 | 0.50 | 0.00 | 3.2 | 1.2 | 2.0 |
| 800 W/m², 25°C | 1.11 | 1.10 | 0.01 | 37.1 | 36.5 | 0.6 |
| 800 W/m², 35°C | 1.50 | 1.50 | 0.00 | 37.5 | 36.5 | 1.0 |
| 500 W/m², 25°C | 2.70 | 2.10 | 0.60 | 75.4 | 75.0 | 0.4 |

At 1000 W/m² and 25°C, the settling time decreased from 0.23 s with PO-MPC to 0.16 s with IN-MPC. This corresponds to a reduction of approximately 30.4%. The tracking error also fell from 3.6% to 2.7%.

When the temperature was increased to 35°C at the same irradiance, both controllers recorded a settling time of 0.50 s. The IN-MPC controller nevertheless produced a lower tracking error of 1.2%, compared with 3.2% for PO-MPC. Thus, the main improvement at this operating point was in tracking accuracy rather than response time. At 800 W/m², the settling-time differences were small. At 25°C, the values were 1.11 s for PO-MPC and 1.10 s for IN-MPC. At 35°C, both controllers recorded 1.50 s. The proposed controller still showed slightly lower tracking errors at both temperatures.

The largest absolute reduction in settling time occurred at 500 W/m² and 25°C. The IN-MPC controller settled in 2.10 s, compared with 2.70 s for PO-MPC. This represents a reduction of 0.60 s, or approximately 22.2%. The difference in the reported tracking error at this condition was comparatively small. These findings show that the improvement provided by IN-MPC was not identical at every operating point. Its clearest benefits were the shorter settling times recorded at 1000 W/m² and 500 W/m² and the lower tracking error obtained at 1000 W/m² at 35°C.

Table 5 summarizes the overall dynamic-performance indices reported for the two controllers.

**Table 5**: Summary of the performance indices of PO-MPC and IN-MPC

| Performance index | PO-MPC | IN-MPC |
|---|---|---|
| Tracking efficiency (%) | 96.9 | 98.8 |
| Settling time (ms) | 100 | 70 |
| Rise time (ms) | 60 | 45 |
| Maximum overshoot (%) | 3.8 | 1.2 |
| Steady-state oscillation (W) | 8.5 | 2.3 |

The proposed controller achieved a tracking efficiency of 98.8%, which was 1.9 percentage points higher than the 96.9% obtained with PO-MPC. Its settling time decreased from 100 ms to 70 ms, representing a 30% reduction, while the rise time decreased from 60 ms to 45 ms. Maximum overshoot fell from 3.8% to 1.2%, indicating that the proposed controller approached the required operating level with a smaller transient departure. Steady-state power oscillation was also reduced from 8.5 W to 2.3 W. This reduction is important because persistent oscillation around the MPP results in repeated movement away from the optimum operating condition and lowers the energy extracted over time.

Overall, the results indicate that the IN-MPC controller provided better transient and steady-state performance than the PO-MPC method in the simulated system. The higher tracking efficiency arose from the combined effect of faster operating-point adjustment, lower overshoot and reduced power fluctuation after convergence. The observed dynamic improvement agrees with the general operating principle of predictive converter control reported by Rodriguez and Cortes (2012) and Vazquez *et al.* (2017). However, the present results specifically show the performance obtained when the predictive switching stage was supplied with a reference voltage generated by the IC algorithm.

## 4. Conclusion

This study developed a hybrid IN-MPC method for MPPT in PV systems. The IC stage generated the reference voltage, while the finite-control-set predictive controller selected the boost-converter switching state that minimized the voltage-tracking error. The proposed controller was implemented in Simulink and compared with a conventional PO-MPC approach under same irradiance, temperature, converter and load conditions.

The results indicate the proposed controller achieved a tracking efficiency of 98.8%, compared with 96.9% for the PO-MPC controller. It also reduced the overall settling time from 100 ms to 70 ms, the rise time from 60 ms to 45 ms, and the maximum overshoot from 3.8% to 1.2%. Steady-state power oscillation decreased from 8.5 W to 2.3 W. Under the low-irradiance test condition of 500 W/m² and 25°C, the settling time was reduced from 2.70 s to 2.10 s.

These results indicate that combining IC reference estimation with predictive switching control improved energy extraction, transient response and steady-state stability in the PV system. The improvement was most evident in the higher tracking efficiency, lower overshoot and reduced power fluctuation around the MPP.

The findings are limited to simulation under uniform irradiance conditions. Experimental validation is therefore required before conclusions can be drawn about real-time implementation. Further work should examine the controller through hardware-in-the-loop and laboratory testing, assess its computational demand on an embedded processor, and evaluate its performance under partial shading, measurement noise, parameter uncertainty and rapidly changing load conditions.

**References**

Abdel-Salam, M., El-Mohandes, MT. and Goda, M. 2018. An improved perturb-and-observe maximum power point tracking algorithm for photovoltaic systems. *Renewable and Sustainable Energy Reviews, 90*: 115–127.

Ahmed, AS., Berzoy, A. and Mohammed, O. 2017. Design and hardware implementation of FL-MPPT control of PV systems based on GA and small-signal analysis. *IEEE Transactions on Sustainable Energy*, 8(1): 279-290.

Alshareef, M., Lin, Z., Ma, M. and Cao, W. 2021. Artificial intelligence-based techniques for maximum power point tracking in photovoltaic systems: A review. *Renewable and Sustainable Energy Reviews, 146*, 111154.

Al-Wesabi, I., Fang, Z., Hussein, HM., Al-shamma'a, AA. and Al-Shaalan, AM. 2024. Comprehensive comparisons of improved incremental conductance with state-of-the-art MPPT techniques. *Energy Reports*, 11: 1590-1610.

Bhagwan, D., Kumar, A. and Singh, B. 2024. Model predictive control-based maximum power point tracking for photovoltaic systems under dynamic environmental conditions. *IEEE Access, 12*, 45873–45888.

Bouzid, AM., Benaissa, B. and Boudour, M. 2020. A comparative study of MPPT techniques for photovoltaic systems under rapidly changing atmospheric conditions. *Solar Energy, 201*: 637–648.

De Soto, W., Klein, SA. and Beckman, WA. 2006. *Improvement and validation of a model for photovoltaic array performance*. Solar Energy, 80(1): 78–88.

Bollipo, RB., Mikkili, S. and Bonthagorla, PK. 2020. Hybrid, optimal, intelligent and classical PV MPPT techniques: A review. *CSEE Journal of Power and Energy Systems*, 7(1), 9-33.Endiz, MS., Gökkuş, G., Coşgun, AE., & Demir, H. (2025). A review of traditional and advanced MPPT approaches for PV systems under uniformly insolation and partially shaded conditions. *Applied Sciences*, *15*(3): 1031.

Esram, T. and Chapman, PL. 2007. Comparison of photovoltaic array maximum power point tracking techniques. *IEEE Transactions on Energy Conversion, 22*(2): 439–449.

Harrison, A., Alombah, NH. and Ndongmo, JD. 2023. A new hybrid MPPT based on incremental conductance–integral backstepping controller applied to a PV system under fast-changing operating conditions. *International Journal of Photoenergy, 2023*, Article 9931481: 1–17.

Hohm, DP. and Ropp, ME. 2003. Comparative study of maximum power point tracking algorithms. *Progress in Photovoltaics: Research and Applications, 11*(1), 47–62.

Kumar, N., Gupta, R. and Pachauri, RK. 2022. Intelligent optimization algorithms for maximum power point tracking of photovoltaic systems: A comprehensive review. *Energy Reports, 8*: 1482–1503.

MathWorks. 2024. *MATLAB and Simulink for renewable energy systems*. https://www.mathworks.com accessed on 27 May, 2026.

Messaoudi, F., Farhani, F. and Zaafouri, A. 2024. A new approach to MPPT hybrid incremental conductance–sliding mode control for PV grid-connected systems. *Measurement and Control*, 57(9): 1370–1382.

Motahhir, S., El Ghzizal, A., Sebti, S. and Derouich, A. 2020. Modeling of photovoltaic systems and maximum power point tracking algorithms. *Solar Energy, 193*: 13–30.

Rashid, MH. 2018. Power Electronics Handbook: Devices, Circuits, and Applications Handbook (4th ed.). Butterworth-Heinemann.

Rivera, M., Toledo, S., Baier, C. and Rodriguez, J. 2021. Model predictive control in power electronics and renewable energy systems: Recent advances and future trends. *IEEE Access, 9*: 17368–17386.

Rodriguez, J. and Cortes, P. 2012. *Predictive Control of Power Converters and Electrical Drives*. Wiley-IEEE Press.

Rodríguez, J., Kazmierkowski, MP., Espinoza, JR., Zanchetta, P., Abu-Rub, H., Young, HA. and Rojas, CA. 2013. State of the art of finite control set model predictive control in power electronics. *IEEE Transactions on Industrial Informatics, 9*(2): 1003–1016.

Vázquez, S., Rodríguez, J., Rivera, M., Franquelo, LG. and Norambuena, M. 2017. Model predictive control for power converters and drives: Advances and trends. *IEEE Transactions on Industrial Electronics, 64*(2): 935–947.

Villalva, MG., Gazoli, JR. and Filho, ER. 2009. Comprehensive approach to modeling and simulation of photovoltaic arrays. *IEEE Transactions on Power Electronics, 24*(5): 1198–1208.

Worku, MY., Hassan, MA., Maraaba, LS., Shafiullah, M., Elkadeem, MR., Hossain, MI. and Abido, M. A. 2023. A comprehensive review of recent maximum power point tracking techniques for photovoltaic systems under partial shading. *Sustainability*, *15*(14): 11132.